DOI: 10.1002/anie.201004601

Where is the Heavy-Atom Effect? Role of the Central Ligand in Tetragold(I) Ethynyl Complexes**

Glenna So Ming Tong, Pui Keong Chow, and Chi-Ming Che**

Triplet excited states have been of great interest for decades, particularly driven by their wide range of applications, including photochemical reactions,[1] photovoltaics,[2] and high-performance organic light-emitting diodes (OLEDs).[3] The triplet manifold is rarely accessed by direct excitation, but is readily populated through intersystem crossing (ISC) from singlet to triplet excited states. ISC is enhanced by the so-called “heavy-atom effect”, which promotes spin–orbit coupling (SOC) between states of different spin multiplicity with an increase in atomic number. Radiative decay of the triplet excited state is also facilitated by the heavy-atom effect. However, the role of the heavy atom in promoting ISC and phosphorescence has recently been questioned. For example, the rate of formation of the ^{3}MLCT (MLCT = metal-to-ligand charge transfer) excited state of $[Re(X)(CO)_3(bpy)]^+$ (bpy = 2,2′-bipyridine) was found to follow the order X = Cl > Br > I,[4] which is contrary to what is expected on the basis of the heavy-atom effect. In most transition-metal complexes, prompt fluorescence from the ^{1}MLCT excited state is generally not observed because of large SOC of the d-block elements, which induces rapid ISC. However, the complexes 2,5-bis(arylethynyl)rhodacyclopentadienes were recently reported to display unusually long-lived, intense fluorescence ($\Phi_F = 0.07$—0.69; $\tau = 3.6$–5.4 ns) despite the presence of a 4d-transition metal ion, Rh^{III}.[5] In addition, it is conceived that the more heavy atoms there are in a complex, the stronger will be the heavy-atom effect, and the faster will be ISC and triplet radiative decay. It has been reported that platinum-containing metallacycles with four and six Pt^{II} ions display ultrafast ISC (in the 100 fs range), but the one with nine Pt^{II} ions shows unexpectedly long ISC lifetime ($\tau = 2.4$ ps).[6] Several years ago, we reported that $[\{TEE\}\{AuPCy_3\}_4]$ (**1**; $\{TEE\}H_4$ = tetraethynylethene; Cy = cyclohexyl) exhibits intense prompt fluorescence ($\Phi_F = 0.22$) but $[\{TEB\}\{AuPCy_3\}_3]$ ($\{TEB\}H_3$ = 1,3,5-triethynylbenzene) displays intense phosphorescence ($\Phi_P = 0.46$) although the former has four Au^I ions and the latter has three.[7]

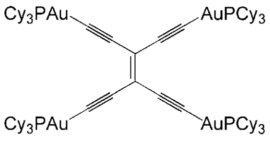

1

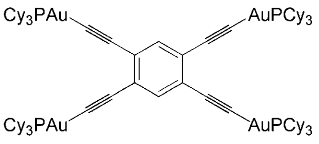

2

So, where is the heavy-atom effect? Herein, we attempt to provide a theoretical rationale using density functional theory (DFT) and time-dependent DFT (TDDFT) to account for the unconventional photophysics of **1**. In addition, we also performed similar calculations on $[\{1245TEB\}\{AuPCy_3\}_4]$ (**2**; $\{1245TEB\}H_4$ = 1,2,4,5-tetraethynylbenzene) to demonstrate how the central ligand (tetraethynylethene vs. tetraethylnylbenzene) plays a decisive role in the photophysics of these tetragold(I) ethynyl complexes. Hereafter, we will use “ethene” and “benzene” as abbreviations for tetraethynylethene and tetraethynylbenzene, respectively.

In brief, spin–orbit coupling matrix elements between singlet and triplet excited states were evaluated within first-order perturbation theory with the assumption that the total spin is a valid quantum number for the complexes studied. Here, only Au^I contributions (both 5d and 6p orbitals) were considered. Computational details are given in the Supporting Information.

To have efficient ISC, the SOC matrix elements between the singlet and triplet excited states should be larger than their energy difference.[8] The TDDFT results of the first 10 singlet and triplet excited states at the optimized singlet ground state geometry of **1** are given in Table S2 of the Supporting Information. In essence, the closest-lying triplet excited state that can couple with S$_1$ excited state is the T$_2$ excited state, which lies approximately 2100 cm^{-1} above the S$_1$ excited state. The S$_1$ and T$_2$ excited states are derived from HOMO→LUMO and HOMO−1→LUMO transitions, respectively. The HOMO has Au($d_{xz}+d_{yz}$) character, whereas HOMO−1 is of Au($d_{xy}+d_{x^2-y^2}$) character. It was found that although each Au ion has significant SOC matrix elements ($|h_{SOC}^x| = 87$–131 cm^{-1} and $|h_{SOC}^y| = 67$–101 cm^{-1}; h_{SOC} refers to the SOC matrix elements of each Au ion and the superscript refers to the spin direction), the total SOC matrix elements (H_{SOC}) when taking into account of all four Au ions are at most 49 cm^{-1} (see Table S3 in the Supporting Information). This “inverse heavy-atom effect” is a consequence of the orbital phases of each Au ion on the MO surfaces of the coupling singlet and triplet excited states (Figure 1, left). For

---

[*] Dr. G. S. M. Tong, P. K. Chow, Prof. Dr. C.-M. Che
State Key Laboratory on Synthetic Chemistry
Institute of Molecular Functional Materials, and
Department of Chemistry, The University of Hong Kong
Pokfulam Road, Hong Kong (China)
Fax: (+86) 852-2857-1586
and
E-mail: tongsm@hku.hk
cmche@hku.hk

[**] We would like to thank the University Development Fund and the AoE (Area of Excellence Scheme) Program of the University of Hong Kong (Project No. [AoE/P-03/08]) for financial support. We also thank the Computer Centre at the University of Hong Kong for providing supercomputers.

Supporting information for this article is available on the WWW under http://dx.doi.org/10.1002/anie.201004601.

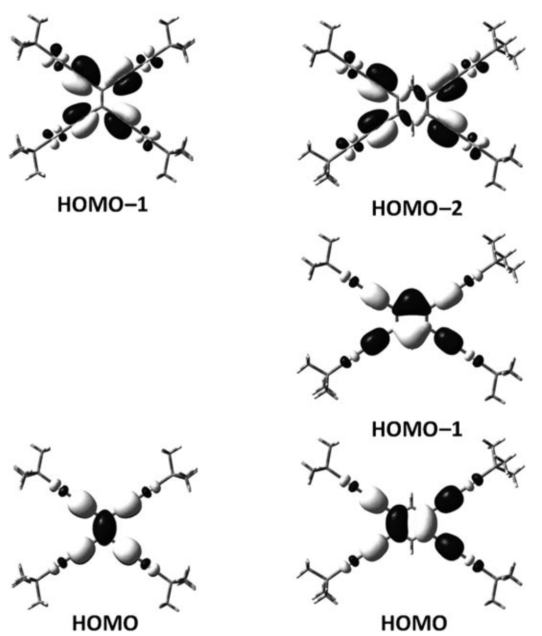

Figure 1. MO surfaces of **1** (left) and **2** (right).

the HOMO, the central bridge ethene is a C=C π-bonding orbital, and all the Au ions have to be of the same phase and symmetric to the mirror plane, σ_{xz}; in contrast, HOMO−1 has no contribution from the central bridge ethene and is antisymmetric to σ_{xz}. As a result, the SOC matrix elements from each Au ion cancel each other, and total $H_{\mathrm{SOC}} < 50\ \mathrm{cm}^{-1} \ll \Delta E(\mathrm{S_1}\text{-}\mathrm{T_2}) \approx 2100\ \mathrm{cm}^{-1}$. ISC is thus sluggish for **1** and is not a good channel to harness its triplet excited states. Hence, prompt fluorescence is observed for this complex.

If the central bridge is changed from ethene to benzene, resulting in complex **2**, the smallest singlet and triplet energy gap that can have spin-orbit coupling is between the S_3 and T_6 excited states (see Table S4 in the Supporting Information). S_3 is made up of HOMO−1→LUMO and HOMO→LUMO+1 transitions, whereas T_6 is predominantly of HOMO−2→LUMO character. Both HOMO and HOMO−1 are of Au(d_{xz}+d_{yz}) character, whereas HOMO−2 has Au(d_{xy}+$d_{x^2-y^2}$) character (Figure 1, right). Now, both HOMO and HOMO−2 are antisymmetric to the mirror plane σ_{xz} such that the SOC matrix elements from each Au ion do not cancel each other, and the total H_{SOC} value along the x direction amounts to 504 cm^{-1}, which is the same order as its energy gap ($\Delta E(\mathrm{S_3}\text{–}\mathrm{T_6}) \approx 270\ \mathrm{cm}^{-1}$). ISC is thus facile and no prompt fluorescence should be observed for **2**. Subsequently, we prepared **2**, which displays strong phosphorescence ($\lambda_{\mathrm{em}} = 532$ nm, $\Phi_{\mathrm{P}} = 0.10$, $\tau = 318$ μs, Figure 2; for experimental details, see the Supporting Information).

The radiative decay rate constant (k_{P}) from the lowest triplet excited state (T_1) is given by Equation (1),[9] where η is the refractive index of the medium, $\chi_k = E(\mathrm{S_k})/E(\mathrm{T_1})$, $E(\mathrm{S_k})$ and $E(\mathrm{T_1})$ are the energies of the kth singlet (S_k) and T_1 excited states, respectively, and f_k is the oscillator strength of the spin-allowed $S_k \rightarrow S_0$ transition; γ refers to the spin direction x, y, or z.

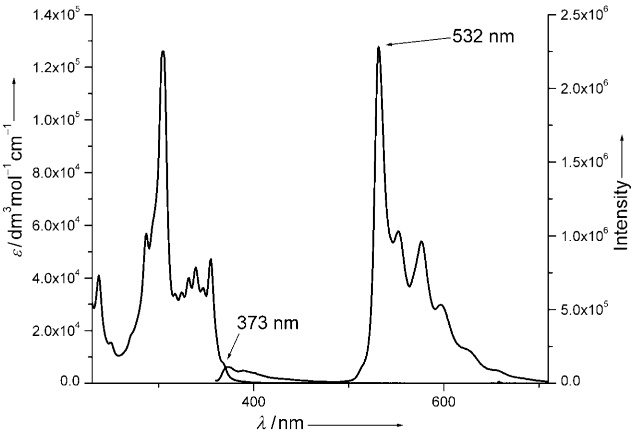

Figure 2. Absorption (left) and emission (right; $\lambda_{\mathrm{ex}} = 365$ nm) spectra of **2**.

$$k_P^{\gamma}(T_1 \rightarrow S_0) = \frac{\eta^2}{1.5}\left\{\sum_k \frac{\langle T_1|H_{\mathrm{SOC}}^{\gamma}|S_k\rangle}{\chi_k^{1/2}(\chi_k - 1)} f_k^{1/2}\right\}^2 = \frac{\eta^2}{1.5}\left\{\sum_k \kappa_{k,P}^{\gamma}\right\}^2 \qquad (1)$$

Tables 1 and 2 list the TDDFT results and the accompanying SOC matrix elements at the optimized T_1 excited states of **1** and **2**, respectively. The following points are noted:

1. Compound **1** has a much lower-lying T_1 state than **2** ($E(\mathrm{T_1}) \approx 6900\ \mathrm{cm}^{-1}$ for the former and $E(\mathrm{T_1}) \approx 14500\ \mathrm{cm}^{-1}$ for the latter); nonradiative decay is thus expected to be faster on the basis of the energy-gap law[10] and the energy ratio is larger for the former (**1**: $\chi_k > 2.8$; **2**: $\chi_k > 1.5$).
2. Although both complexes are of high symmetry (pseudo-D_{2h}), **1** has no strongly allowed low-lying $S_k \rightarrow S_0$ transitions ($f_k < 1.0$ for $k = 1$–10), whereas **2** has a strongly allowed $S_3 \rightarrow S_0$ transition ($f_3 = 2.4184$) and S_3 can undergo SOC with T_1 excited state.

Table 1: Nature and excited state parameters of **1**.[a,b]

	Nature (CI coefficients)	E [cm^{-1}]	f_k	χ_k	$\langle T_1 \mid H_{\mathrm{SOC}}^{\gamma} \mid S_k\rangle$ [cm^{-1}]	$\kappa_{k,\mathrm{P}}$ [s^{-1}]
T_1	HOMO→LUMO (1.00681)	6920	0.0000	–	–	–
S_1	HOMO→LUMO (0.60619)	19757	0.7997	–	–	–
T_2	HOMO−1→LUMO (0.71016)	23243	0.0000	–	–	–
S_3	HOMO→LUMO+1 (0.70021)	27172	0.0001	3.93	247[c]	0.427
S_8	HOMO→LUMO+4 (0.69159)	29368	0.3389	4.24	−1.14[d]	0.009

[a] Only key excited states mentioned in the text are given here. A full list of the first 10 singlet and triplet excited state properties is presented in the Supporting Information. [b] The tabulated results were obtained at the T_1 optimized geometry. [c] Along the y direction. [d] Along the z direction without CI coefficients taken into account.

Table 2: Nature and excited state parameters of **2**.[a,b]

	Nature (CI coefficients)	E [cm^{-1}]	f_k	χ_k	$<T_1\|H_{SOC}{}^{\gamma}\|S_k>$ [cm^{-1}]	$\kappa_{k,P}$ [s^{-1}]
T_1	HOMO→LUMO (0.78878)	14482	0.0000	–	–	
T_2	HOMO−1→LUMO (0.61171) HOMO→LUMO+1 (−0.39176)	22591	0.0000	–	–	–
S_1	HOMO→LUMO (0.64578)	23736	0.7188	–	–	–
S_2	HOMO−1→LUMO (0.51541) HOMO→LUMO+1 (0.47973)	27031	0.0103	1.56	7.65[c]	0.110
S_3	HOMO−1→LUMO (−0.42824) HOMO→LUMO+1 (0.49013)	29659	2.4184	2.05	7.65[c]	−3.05

[a] Only key excited states mentioned in the text are given here. A full list of the first 10 singlet and triplet excited state properties is presented in the Supporting Information. [b] The tabulated results were obtained at the T_1 optimized geometry. [c] Along the *z* direction without CI coefficients taken into account.

3. Although H_{SOC} between T_1 and S_3 is large (247 cm^{-1} with both MLCT and LMCT contributions) for **1** and small (7.56 cm^{-1} with only MLCT contributions) for **2**, the $S_3 \rightarrow S_0$ transition for the former is almost symmetry forbidden ($f_3 = 0.0001$), whereas the latter is strongly allowed ($f_3 = 2.4184$); together with the smaller energy ratio ($\chi_3 = 2.05$ and 3.93 for **2** and **1**, respectively), $T_1 \rightarrow S_0$ radiative decay rate constant is two orders of magnitude faster with **2**.

Thus, it is neither the high symmetry nor the number of Au^I ions that governs the photophysics of these tetragold(I) ethynyl complexes. Rather, the central ligand plays a decisive role. The T_1 excited state is very low-lying with ethene as the central ligand, whereas it is moderately low (in the deep red region) when benzene is the central bridge. This result could be readily understood by the fact that triplet biradical is a stable configuration for the ethene moiety with which the overlap between the C(pπ) orbitals are weak (the C–C distance of the ethene moiety is much longer at the optimized T_1 excited state: 1.514 Å; Wiberg bond index = 1.4455 for S_0 and 0.9697 for T_1).[8] It has also been shown by Ottosson and co-workers that both fulvenes and fulvalenes also have low-lying T_1 and Q_1 excited states, respectively.[11] However, the benzene moiety is aromatic in its S_0 state and, according to Baird's theory,[12] the T_1 excited state is antiaromatic and thus the T_1 excited state of **2** is relatively higher lying than that of **1**. Moreover, as there are more π and π* orbitals for benzene (six in total for the benzene bridge and only two for the ethene bridge), there are more allowed low-lying singlet transitions (in particular, S_2 and S_3 excited states for **2**) for T_1 excited state to borrow intensity from. Thus, **1** displays prompt fluorescence, whereas **2** exhibits intense phosphorescence.

Is it then possible to utilize the T_1 excited state of **1**? It is noted that besides ISC, triplet excited states can also be produced by singlet fission, whereby a singlet exciton splits into two triplet excitons. This phenomenon is particularly attractive to dye-sensitized solar cells, as two charge carriers are created from a single absorbed photon by singlet fission, thus doubling the solar cell efficiency. Nozik, Ratner, Michl and co-workers pointed out that biradicals are likely candidates for singlet fission with a favorable excited state ordering of $E(T_2)$, $E(S_1) > 2E(T_1)$.[13] In addition, for an ideal Grätzel cell, the optimum values are $E(S_1) \approx 1.8$–2.2 eV and $E(T_1) \approx 0.9$–1.1 eV. From the TDDFT results in Table S4, it can be seen that the excited-state energies of complex **1** meet the forementioned energetic requirements for efficient dye-sensitized solar cells: $E(T_2) \approx 23200$ cm^{-1} (≈ 2.89 eV), $E(S_1) \approx 19800$ cm^{-1} (≈ 2.45 eV) $> 2E(T_1) \approx 13800$ cm^{-1} ($E(T_1) \approx 0.86$ eV). Hence, **1** may be a good candidate for solar-cell applications.

From the present analysis, it was demonstrated that the choice of the central ligand is critical in tuning the photophysics of transition-metal complexes. The heavy-atom effect is not the sole factor that determines the efficiency of intersystem crossing and triplet radiative decay rate. Knowledge of the electronic structure and symmetry of the MO surfaces responsible for the SOC is also indispensable in device design. $[\{TEE\}\{AuPCy_3\}_4]$ (**1**) is a "chameleon" that can utilize its singlet excited state when applied as a fluorescent OLED but its triplet excited state when applied to photovoltaics.

Received: July 27, 2010
Published online: October 22, 2010

Keywords: density functional calculations · gold · luminescence · photophysics

---

[1] a) A. Vlček, Jr., *Top. Organomet. Chem.* **2010**, *29*, 73–114; b) M. Sakamoto, T. Tachikawa, M. Fujitsuka, T. Majima, *Langmuir* **2009**, *25*, 13888–13893; c) K. Plaetzer, B. Krammer, J. Berlanda, F. Berr, T. Kiesslich, *Lasers Med. Sci.* **2009**, *24*, 259–268; d) C. M. Che, S. W. Lai, *Coord. Chem. Rev.* **2005**, *249*, 1296–1309; e) C. Schweitzer, R. Schmidt, *Chem. Rev.* **2003**, *103*, 1685–1757; f) S. Tero-Kubota, A. Katsuki, Y. Kobori, *J. Photochem. Photobiol. C* **2001**, *2*, 17–33.

[2] a) W.-Y. Wong, C.-L. Ho, *Acc. Chem. Res.* **2010**, *43*, 1246–1256; b) T. A. Clem, D. F. J. Kavulak, E. J. Westling, J. M. J. Fréchet, *Chem. Mater.* **2010**, *22*, 1977–1987; c) G. L. Schulz, S. Holdcroft, *Chem. Mater.* **2008**, *20*, 5351–5355; d) J. Michl, A. J. Nozik, X. Chen, J. C. Johnson, G. Rana, A. Akdag, *Proc. SPIE* **2007**, 66560E-66561-66569.

[3] a) H. Yersin, *Highly Efficient OLEDs with Phosphorescent Materials*, Wiley-VCH, Weinheim, **2008**, p. 259; b) A. F. Rausch, H. H. H. Homeier, H. Yersin, *Top. Organomet. Chem.* **2010**, *29*, 193–235; c) L. Murphy, J. A. G. Williams, *Top. Organomet. Chem.* **2009**, *28*, 75–111; d) F. Laquai, Y.-S. Park, J.-J. Kim, T. Basche, *Macromol. Rapid Commun.* **2009**, *30*, 1203–1231; e) Y. You, S. Y. Park, *Dalton Trans.* **2009**, 1267–1282; f) W.-Y. Wong, C.-L. Ho, *J. Mater. Chem.* **2009**, *19*, 4457–4482; g) Z. M. Hudson, S. Wang, *Acc. Chem. Res.* **2009**, *42*, 1584–1596; h) R. C. Evans, P. Douglas, C. J. Winscom, *Coord. Chem. Rev.*

2006, *250*, 2093 – 2126; i) S. W. Lai, C. M. Che, *Top. Curr. Chem.* **2004**, *241*, 27 – 63.

[4] A. Cannizzo, A. M. Blanco-Rodríguez, A. E. Nahhas, J. Šebera, S. Záliš, A. Vlček, Jr., M. Chergui, *J. Am. Chem. Soc.* **2008**, *130*, 8967 – 8974.

[5] A. Steffen, M. G. Tay, A. S. Batsanov, J. A. K. Howard, A. Beeby, K. Q. Vuong, X.-Z. Sun, M. W. George, T. B. Marder, *Angew. Chem.* **2010**, *122*, 2399 – 2403; *Angew. Chem. Int. Ed.* **2010**, *49*, 2349 – 2353.

[6] D. C. Flynn, G. Ramakrishna, H.-B. Yang, B. H. Northrop, P. J. Stang, T. Goodson III, *J. Am. Chem. Soc.* **2010**, *132*, 1348 – 1358.

[7] W. Lu, N. Zhu, C.-M. Che, *J. Organomet. Chem.* **2003**, *670*, 11 – 16.

[8] L. Salem, C. Rowland, *Angew. Chem.* **1972**, *84*, 86 – 106; *Angew. Chem. Int. Ed. Engl.* **1972**, *11*, 92 – 111.

[9] G. S. M. Tong, C.-M. Che, *Chem. Eur. J.* **2009**, *15*, 7225 – 7237.

[10] R. Englman, J. Jortner, *Mol. Phys.* **1970**, *18*, 145 – 164.

[11] H. Möllerstedt, M. C. Piqueras, R. Crespo, H. Ottosson, *J. Am. Chem. Soc.* **2004**, *126*, 13938 – 13939.

[12] N. C. Baird, *J. Am. Chem. Soc.* **1972**, *94*, 4941 – 4948.

[13] I. Paci, J. C. Johnson, X. Chen, G. Rana, D. Popovic, D. E. David, A. J. Nozik, M. A. Ratner, J. Michl, *J. Am. Chem. Soc.* **2006**, *128*, 16546 – 16553.